RSC Advances

Attachment Based Growth: Building Architecturally Defined Metal Nanocolloids Particle by Particle

Journal:	*RSC Advances*
Manuscript ID:	RA-REV-04-2015-007156
Article Type:	Review Article
Date Submitted by the Author:	20-Apr-2015
Complete List of Authors:	Skrabalak, Sara; Indiana University - Bloomington, Chemistry Ataee-Esfahani, Hamed; Indiana University,

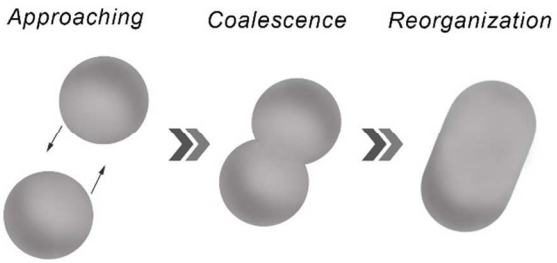

This review highlights the principles and recent mechanistic insight into the synthesis of metal nanostructures using nanoparticles as primary building blocks.

RSC Advances

RSCPublishing

REVIEW

Attachment Based Growth: Building Architecturally Defined Metal Nanocolloids Particle by Particle

Cite this: DOI: 10.1039/x0xx00000x

Received 00th January 2012,
Accepted 00th January 2012

DOI: 10.1039/x0xx00000x

www.rsc.org/

Hamed Ataee-Esfahani[a] and Sara E Skrabalak[a*]

Recent mechanistic insight into the synthesis of metal nanostructures by attachment-based growth is highlighted in this review. From quasi-spherical particles to nanowires, nanodendrites, and heterostructures built from nanoparticles as primary building blocks, the principles of oriented and misoriented attachment of metal nanoparticles are discussed within the context of diverse synthetic conditions. From this survey, a greater understanding of this growth mechanism emerges to provide general, and potentially greener, principles for the synthesis of advanced metal nanostructures, including those with applications in catalysis.

1. Introduction

Incredible advances in nanomaterial synthesis are enabling the design of nanocolloids with unique physicochemical properties that are tailored to address diverse scientific needs.[1,2] For example, metal nanocolloids are being studied as catalysts for different reactions, with enhanced rates of reaction achieved as a function of colloid size.[2] Beyond their intrinsic catalytic activity, the performance of metal nanocolloids can be enhanced by manipulation of their composition and architecture (*e.g.*, binary or ternary metallic nanostructures in the form of an alloy or core@shell distribution).[3,4] However, strategies towards the sustainable synthesis of nanomaterials need to be addressed to bridge these laboratory-scale achievements to industrial use.

Just as in the synthesis of organic compounds where tenets of high atom economy and green routes to compounds are preferred,[5] the nanomaterial synthesis community must strive to develop cleaner and more sustainable methods for the synthesis of advanced nanomaterials. Examples of current limitations include reliance on organic compounds as solvent and/or structure-directing agents (often surfactants and polymers), low synthesis efficiency through the formation of byproducts and lack of reagent recycling, and high temperature or pressure synthetic conditions.[6] To address these limitations, a better understanding of nucleation and growth mechanisms and effective parameters to direct the evolution of nanocrystal size and shape are required. Classically, nanocrystal growth proceeds through atomic addition to crystallographic facets, along with Ostwald ripening. In 1998, Penn and Banfield reported oriented attachment as a new mechanism for crystal growth.[7] In this process, crystals grow through self-organization and coalescence of adjacent nanocrystals. Attachment-based growth can break the symmetry of crystals, opening the door for the synthesis of anisotropic nanostructures. Attachment-based growth also provides a new synthetic framework in which organic additives may not be required to direct crystal formation; this ability is rarely possible in classical overgrowth systems where surfactants or polymers are needed to tune crystallite size and morphology. Hence, attachment-based growth could offer a paradigm for greener nanomaterial syntheses. Although this growth mechanism was first observed in and applied to the synthesis of metal oxides and other semiconductors,[7] oriented attachment has recently been implicated in the synthesis of metal nanostructures. Here, recent advances in the attachment-based synthesis of metal nanostructures and their catalytic properties are reviewed. The principles that underlie metal nanocrystal growth by oriented and misoriented attachment are introduced in Section 2. Then, a survey of metal nanostructures achieved by these mechanisms is provided in Section 3. These examples begin to provide a framework for the design of metal nanostructures through particle coalescence. Section 4 concludes with the synthesis of multicomponent metal nanostructures (*e.g.* dimers and core@shell nanoparticles) by attachment-based growth, with

[a] Dr. H. Ataee-Esfahani, Prof. S. E. Skrabalak
Department of Chemistry
Indiana University - Bloomington
800 E. Kirkwood Ave. Bloomington, IN 47405, USA
E-mails: sskrabal@indiana.edu (S.E.S),
hameatae@indiana.edu (H.A.)
Homepage: http://www.indiana.edu/~skrablab/

these structures representing functional nanomaterials in many cases.

2. Classical Overgrowth *versus* Attachment-based Growth

Solution phase synthesis of metal nanoparticles can be categorized based on their initial building blocks, *i.e.,* atoms or nanoparticles.[8] In the case of atomic building blocks, nanoparticle growth is accounted for by the addition of atoms to the highest energy features of seeds, which leads to their fast growth and eventual disappearance. This condition leads to nanostructures with thermodynamically favorable shapes, *i.e.,* bounded by low surface energy facets. Deviations through kinetically controlled overgrowth are also possible, and both topics have been reviewed in detail elsewhere.[6]

In the case of nanoparticles as building blocks, colloids with a high collision-stick frequency attach to one another, instead of atoms, and lead to an increase in nanostructure size. This mechanism of crystal growth includes the self-organization of neighboring nanoparticles in mutual orientation and subsequent collision and coalescence, *i.e.,* oriented attachment where merging two nanocrystals results in a new single crystal.[9,10] The structural characteristics of the product depend on the capacity of the colliding nanoparticles for self-organization at mutual orientation. In the case of small misalignment, coalesced nanoparticles can preserve single crystallinity through reorientation upon contact[9] and/or diffusion of atoms and the gradual disappearance of defects during structural relaxation.[10] However, if misalignment is high and coalescence occurs, defects will be generated at the interface and the process is called misoriented attachment.[9] In both oriented and misoriented attachment, the total surface energy decreases by elimination of facets shared in the coalescence process. As discussed in Section 3 and 4, these mechanisms facilitate the creation of highly branched and anisotropic nanostructures.[11]

From the view point of thermodynamics, the major driving force for the coalescence of nanoparticles is reduction of surface energy. Attachment of two nanoparticles eliminates their interface and decreases the total surface energy.[12] In crystalline materials, different facets have different surface energies, and attachment is assumed to occur preferentially on surfaces with higher energy to maximize this energy reduction. This assumption is in good agreement with experimental observations presented in Section 3. On the other hand, surfactants, polymers, and ions can stabilize crystallographic facets by adsorption.[6] Thus, tuning the surface energies of facets through structure-directing agents can be used as an effective tool to guide the attachment of nanocolloids, as discussed also in Section 3.

The interaction strength between nanoparticles is key to determining whether or not nanoparticle attachment occurs.[13,14] Columbic repulsion can prevent the attachment of approaching nanoparticles. This repulsive force depends on the magnitude of columbic interaction between nanoparticles, which arises from their surface charge. Zeta (ζ) potential measurements can be used as an indicator of surface charge. A minimum ζ potential of $\pm$30 mV provides enough repulsive force to keep particles stable in colloidal suspensions.[14,15] Still, attractive forces between nanoparticles, such as van der Waals and dipolar interactions, can facilitate attachment.[8,16,17] Although relevant in semiconductor nanoparticles, dipolar interactions between metal nanoparticles are negligible in most cases as long lived dipoles are unlikely in metals due to their free electron clouds.[18] However, electric dipoles can be created with the aid of surfactants and other ligands adsorbed on the surfaces of metal colloids.[8,16]

The competition between these attractive and repulsive interactions contribute to the attachment kinetics, with coalescence achieved when attractive interactions dominate. As illustrated with the following examples, these mechanisms of attachment are not limited to the growth of single-component nanostructures. Multicomponent architectures are possible when attachment involves nanoparticles with different compositions and/or structure. Here, recent advances in the synthesis of both single-component (*i.e.,* monometallic and alloyed) and multicomponent (*i.e.,* dimers and core@shell) nanostructures through attachment-based growth are reviewed.

3. Attachment-based Synthesis of Single-Component Nanostructures

As discussed in Section 2, the attachment of nanoparticles does not always create a coherent interface, and defects (*e.g.,* twin planes, grain boundaries, etc.) can be introduced if the colliding nanoparticles are not aligned appropriately.[9] Advancements in electron microscopy are enabling crystal growth to be monitored in real-time, in solution-phase.[19,20] In the case of metal nanostructures, Mirsaidov *et al.* studied the coalescence of 10 nm Au nanocrystals in solution, providing insight into growth by attachment.[9] As shown in Figure 1a, they classified nanocrystal attachment to either defect-free or defect-mediated pathways, which were found to depend on the degree of lattice alignment between colliding particles as defined by a critical angle. In the case of 10 nm Au nanocrystals, this critical angle was around 15°. As shown in Figure 1b, the attachment of three nanocrystals was monitored in which the nanocrystals designated P and Q coalesce through a common (111) crystallographic plane, leading to a defect-free single crystal (PQ), where the original particles are bridged by a neck (t=5.9s, t=69.1s). Eventually, (at t=75.2s) the nanocrystal designated R approaches the PQ crystal, with attachment proceeding through (200) and (111) planes. This misalignment creates defects at the R-PQ crystal interface (t=135.9s). In both collisions, the neck areas and voids between the fused nanocrystals are filled by diffusion of surface atoms. As shown in Figure 1c and d, a molecular dynamics (MD) simulation also supports energy reduction as the driving force for attachment in spite of defects being introduced during attachment.[9]

Alivisatos *et al.* studied the growth mechanism of Pt nanoparticles by *in situ* liquid cell TEM and found both cluster attachment and atomic addition contribute to nanoparticle growth.[20] Interestingly, following the coalescence of clusters, structural reorganization was observed to yield single-crystalline Pt nanoparticles while atomic addition ensured a narrow size distribution.[10,19] The imaging also revealed that coalescence occurred between (111) facets. Although {111} facets are lowest in energy for face centered cubic metals, the collision at these facets was explained by lower ligand coverage, modifying the relative surface energies. Tracking the clusters before coalescence showed a period of correlated motions which facilitated lattice alignment. This motion likely arises from the attractive and repulsive forces between nanoparticles, as mentioned in the Introduction. Misoriented attachment of Pt nanocrystals was also reported, which produced twin boundaries

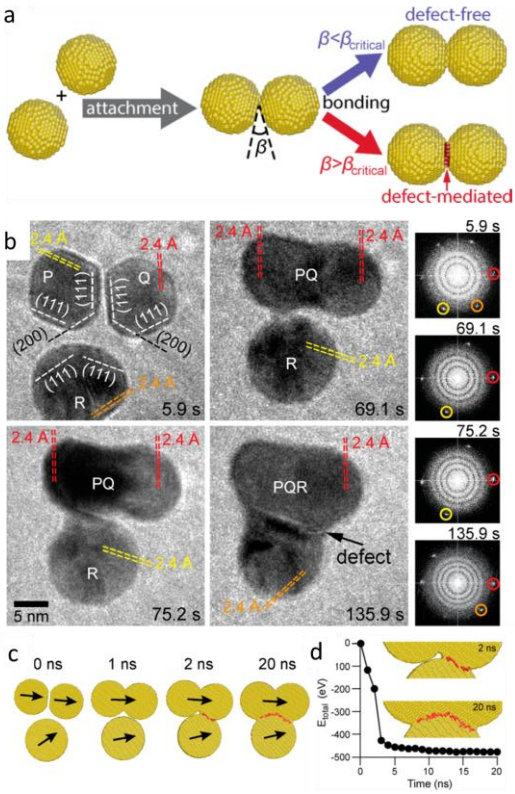

Figure 1. a) Schematic of nanoparticle attachment and formation of coherent and defect-mediated interfaces. b) TEM images of the coalescence events between three 10 nm Au nanocrystals (designated P, Q, and R). The observed lattice fringes are indicated by the dashed lines and corresponding Fourier reflections of (111) planes. c) A MD simulation of the coalescence of three 10 nm gold nanocrystals. Defects in the nanocrystals are highlighted by red atoms. d) Plot of total energy change during the coalescence of the three nanocrystals. Inset is a zoomed in view of the interface between the nanocrystals shown in c). (adapted from Reference 9)

which were preserved even after structural reorganization.[20] These studies reveal the general principles behind oriented and misoriented attachment. Although common in the synthesis of quasi-spherical particles, these processes can lead to a break in symmetry and the formation of metal nanowires and nanodendrites, as discussed in the Sections 3.1 and 3.2.

3. 1. Attachment-based Growth of Nanowires

As evident in Figure 1 with the attachment of nanocrystals P and Q, end-to-end attachment of small nanoparticles can occur. When this process proceeds multiple times over, chain-like or nanowire structures can form. Ravishankar *et al.* studied the solution phase synthesis of Au nanowires in the presence of oleylamine, oleic acid, and ascorbic acid at 120 °C.[21] Au nanowires with diameters of 2 nm and lengths of about 1 μm were prepared by fusion of the (111) facets of adjacent Au nanocrystals. Just as in the study of quasi-spherical Pt nanocrystal formation, coalescence through the (111) facets was attributed to a ligand effect. In this case, the amine capping agent was cited to have weaker binding affinity and fewer sites for adsorption on {111} facets compared to {100} facets, which were also expressed by the Au nanocrystal building blocks. Still, a symmetry-breaking mechanism is required to achieve nanowire growth by attachment as there are several equivalent {111} facets on each nanocrystal which could yield branched or dendritic nanostructures instead. As shown in Figure 2a, attachment of two quasi-spherical nanocrystals can create a necked interface. This structure introduces a difference in chemical potential because of the alternating concave and convex surfaces, leading to surface diffusion of atoms. This phenomenon, called smoothing, transforms rough (faceted) surfaces to smooth (curved) surfaces; in turn, nanocrystal attachments proceed selectively to the (111) facets at the ends (Figure 2b). Shown in Figure 2c is a TEM image of the resultant Au nanowires.[21] In addition to Au nanowire formation[22,23], the synthesis of Ag[24,25], Pt[26,27], and Pd[28] nanowires have been reported to proceed through a similar attachment mechanism.
Similar to monometallic nanoparticles, alloyed nanoparticles can

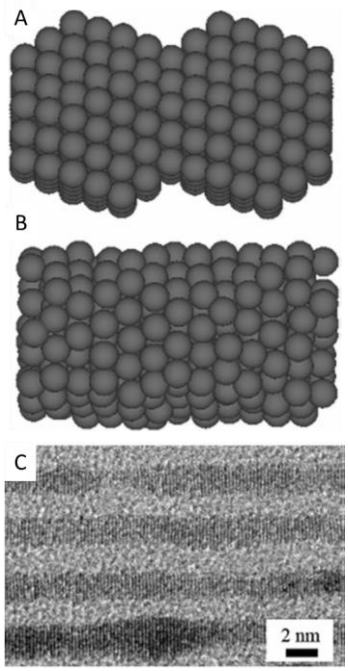

Figure 2. A schematic of the smoothing process which leads to symmetry-breaking and the formation of nanowires by attachment. In a), the alternating concave and convex regions are smoothed out by diffusion b). In a), there are 4 {111} facets available for attachment whereas in b) there is only one facet along the growth direction. c) High-resolution TEM image of Au nanowires. (adapted from Reference 21)

interact and coalesce to reduce their surface energy, producing nanowires or branched nanostructures. However, Yang *et al.* found that the tendency towards oriented attachment depends on the composition of the building block nanoparticles.[29] To study the effect of composition, pure Pt, pure Ag, and alloyed $Pt_{53}Ag_{47}$ nanostructures were prepared in the presence of oleic acid and oleylamine under otherwise identical synthetic conditions. As shown in Figures 3a and b, the monometallic systems produced quasi-spherical Pt or Ag nanoparticles. In contrast, the alloyed system produced wormlike nanowires. TEM analysis of reaction aliquots supports an attachment growth mechanism for nanowire formation while the quasi-spherical particles are consistent with

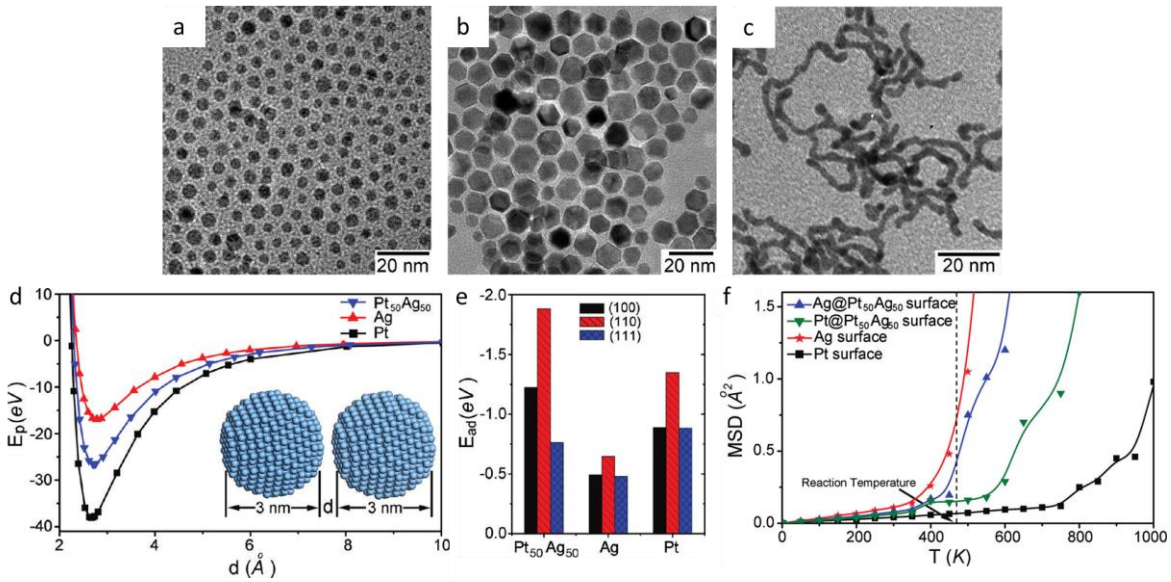

Figure 3. TEM images of a) Ag nanoparticles, b) Pt nanoparticles and c) $Pt_{53}Ag_{47}$ nanowires obtained under the same condition. d) Potential energy (E_p) as a function of distance between two Pt, two $Pt_{50}Ag_{50}$, and two Ag nanoparticles. e) Adsorption energy (E_{ad}) of oleylamine (OAm) molecules on the three low index surfaces of $Pt_{50}Ag_{50}$, Ag, and Pt. f) Simulation of mean square displacement of surface atoms of 3 nm Ag, PtAg alloys, and Pt nanoparticles. (adapted from Reference 29)

classical overgrowth. To better understand this compositional effect, MD and density functional theory (DFT) simulations analyzed the effect of composition on the interaction and attachment of nanocrystals. The potential energy (E_p) between two Pt, two $Pt_{50}Ag_{50}$ (to mimic the $Pt_{53}Ag_{47}$ nanowire system), and two Ag nanoparticles was simulated as a function of distance by the MD method (Figure 3d). The minimum E_p obtained in all three systems arose when particles were in close contact, and the potential energy gained upon collision provides a driving force for attachment. This gain is smallest for Ag, which is in good agreement with TEM showing quasi-spherical Ag nanoparticles consistent with classical overgrowth (Figure 3a). However, considering the Pt and $Pt_{50}Ag_{50}$ systems, interpretation is not as straightforward as this gain in potential energy is greatest for the Pt system which also produced spherical particles consistent with classical overgrowth. To account for this observation, the effect of adsorbates on surface energy was considered.

Specifically, the adsorption energies of propylamine and propanoic acid on the (111), (110), and (100) surfaces of Ag, Pt, and $Pt_{50}Ag_{50}$ were simulated by DFT. These molecules were selected to simplify the simulation while still examining the influence of the key functional groups (amine and carboxylic acid) involved in surface adsorption by the capping agents present. The amine was found to bind more strongly than the carboxylic acid. Its adsorption strength was weakest on (111) surfaces, leaving them less protected by capping agents. Interestingly, the adsorption strengths of the amine on Ag surfaces were less than either Pt or $Pt_{50}Ag_{50}$; this finding indicates again that a low potential energy gain inhibits particle-particle coalescence. With this insight, another parameter must be considered to account for Pt nanoparticle and wormlike $Pt_{53}Ag_{47}$ nanowire formation. In addition to these thermodynamic parameters, reconstruction of interface atoms upon collision to form strong metallic bonds is important. MD simulations were used to obtain the mean square displacements (MSDs) for atoms in the Ag, Pt, and $Pt_{50}Ag_{50}$ systems. The results showed that Ag can easily diffuse at the $Pt_{50}Ag_{50}$ particle interfaces, whereas Pt does not at Pt particle interfaces (Figure 3f). This feature would make Pt-Pt bond breaking and reconstruction at interfaces unlikely, inhibiting coalescence despite potential energy analysis indicating that Pt-Pt particle attachment is thermodynamically favorable. These simulations and experimental findings illustrate the competing thermodynamic and kinetic factors that account for the composition and structure of metal colloids assembled through particle attachment.[29]

Just as the diffusion of atoms contribute to nanowire formation in monometallic systems, this process is important to nanowires formed from the coalescence of alloyed nanoparticles. However, in addition to this atomic reorganization eliminating structural defects, atomic diffusion can improve compositional uniformity in multimetallic systems. Zheng *et al.* reported the oriented attachment of Pt_3Fe nanocrystals into nanorods driven by dipolar interactions.[8] As discussed in Section 2, the formation of electrostatic dipoles was attributed to the stored charge in adsorbed surfactants, which repelled side-to-side attachment and instead facilitated end-to-end contact. *In situ* liquid cell TEM was used to study the growth of these nanorods in real time. Figure 4 shows sequential images of the preferential attachment of nanoparticles to the end of a chain of nanoparticles. First, small Pt_3Fe nanoparticle chains form by attachment of adjacent nanoparticles. Then, longer and twisted polycrystalline chains are created by end-to-end attachment of the initial small chains (Figure 4A). This assembly process is followed by straightening and reorganization of the nanocrystalline domains to yield straight, single-crystalline nanorods. This reorganization and straightening is driven by a reduction in total energy through elimination of defects and a reduction in surface energy. Interestingly, the authors noted that iron-rich regions (marked by arrows in Figure 4B) were diminished through this structural relaxation process.[8] Different alloyed nanostructures including nanowires (*e.g.* PdPt[30-33], PdAg[30], PdPtAg[30], PtRh[34], AuAg[35],

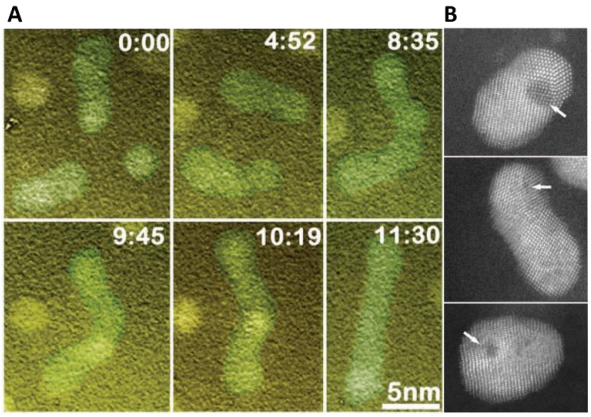

Figure 4. a) Sequential TEM images of the growth of a Pt_3Fe nanorod. b) High-angle annular dark field (HAADF) STEM image of a polycrystalline Pt_3Fe nanoparticles. Arrows indicate the iron-rich regions (dark spots). (adapted from Reference 8)

PdCu[36], PtFe[8], PtAg[29], AuPd[37], PtRu[38]) have been synthesized by co-reduction of different metal salts coupled with growth by oriented attachment.

Interestingly, the attachment mechanism which accounts for nanorod and nanowire formation can be reversed through the use of etchants. As discussed at the beginning of Section 3, coalescence of nanoparticles at high angles introduces defects at the particle-particle interface. These defects are susceptible to oxidative etching, which can lead to fragmentation. For example, Han *et al.* found that Pd and Pt nanowires synthesized from precursor solutions containing $Pd(NO_3)_2$ or $PtCl_2$ can be transformed to nearly spherical nanoparticles when air is bubbled through the reaction solution and kept open to air for 12 hours.[39] This transformation occurs because twin boundaries and stacking faults are active sites for oxygen absorption, and etching preferentially initiates at these high energy defects to separate the structure into smaller units.[39]

3. 2. Attachment-based Growth of Nanodendrites

As illustrated with the examples of nanorod and nanowire formation, reduction in surface energy is a key factor facilitating attachment of metal nanoparticles. Considering the case of truncated octahedral metal nanocrystals, these nanocrystals are bound by eight (111) facets and six (100) facets; with the assumption that (100) facets are higher in energy, there are thus six facets with an equal chance of attachment. As discussed in Section 3.1, induced dipolar moments by adsorbents or fast diffusion of surface atoms (*i.e.*, smoothing) can direct the formation of nanowires through end-to-end attachment of nanoparticles. However, in many colloidal syntheses, these conditions do not dominate and higher order structures such as metal nanodendrites would be expected through attachment.

Nanodendrites have been made of different metals, including Pt[40-48], Pd[49-52], Rh[53], and Ag[54,55]. With respect to morphology, nanodendrites range from multi-armed nanoparticles with an open structure to large bundles made of closely packed particles. They may be single-crystalline or polycrystalline. The specific nanodendritic morphology can be rationalized in terms of the concentration of initial building blocks (*i.e.*, the smaller nanoparticles which attach to give the final branched structure) as well as the type and concentration of ligands, surfactants, and other additives in a synthesis.

Recently, we studied the influence of metal-ligand interactions in attachment-based growth.[50] Specifically, Pd nanostructures were synthesized by heating Pd precursors with different local ligand environments in oleylamine, which served as both a capping agent and reducing agent. Different nanostructures were obtained by manipulating the ligands in the synthesis. For example, the use of palladium acetylacetonate ($Pd(acac)_2$) yielded multi-armed Pd nanodendrites, whereas the use of palladium hexafluoroacetylacetonate ($Pd(hfac)_2$) yielded larger Pd bundles (Figure 5). The higher aggregation level of Pd nanoparticles and formation of Pd bundles was attributed to the faster generation of Pd nanoparticles on account of the better leaving-group properties of the $hfac^-$ ligands compared to $acac^-$. These nanodendrites and bundles were polycrystalline, indicating the formation of defects at the interface upon attachment due to misorientation between colliding

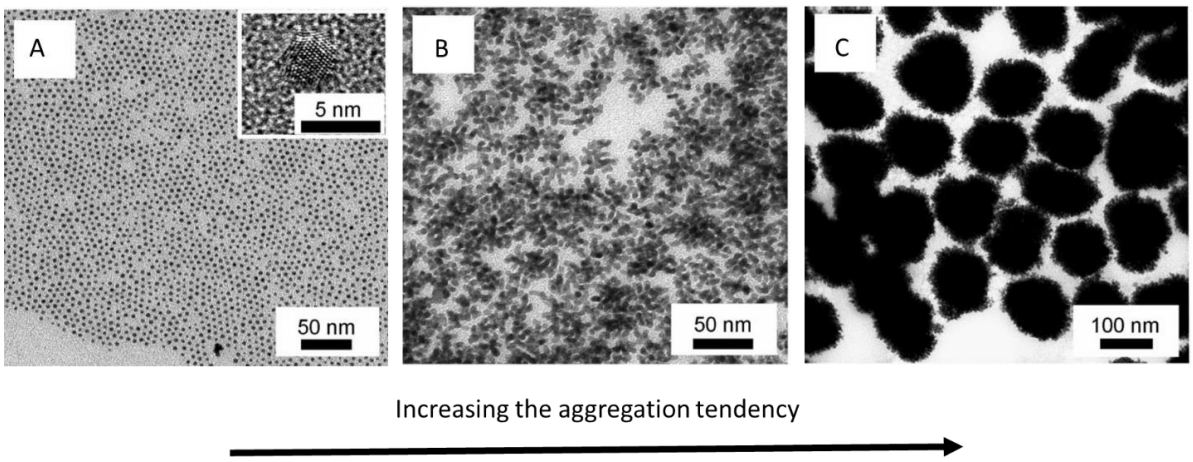

Figure 5. TEM images of a) spherical Pd nanocrystals obtained by heating $Pd(acac)_2$ in TOP and oleylamine, b) Pd nanodendrites prepared by heating $Pd(hfac)_2$ in oleylamine, and c) Pd bundles formed by heating $Pd(acac)_2$ in oleylamine. (adapted from Reference 50)

nanoparticles. Interestingly, the addition of strongly coordinating ligands such as trioctylphosphine (TOP) led to the production of quasi-spherical nanoparticles. This occurrence was attributed to the greater binding affinity between the phosphine ligands and the surfaces of Pd nanoparticles. In surveying other precursors (*e.g.*, palladium acetate ($Pd(OAc)_2$) and phase-transferred sodium tetrachloropalladate (Na_2PdCl_4)) as a Pd source and other additives (e.g. triphenylphosphine (PPh_3)), we concluded that ligands with intermediate binding affinity towards metal ions regulate their gradual reduction and promote the assembly of weakly passivated Pd nanoparticles into nanodendrites or nanobundles. In contrast, strongly coordinated ligands slow the nucleation rate and yield well-passivated nanoparticles which grow by atomic addition.[50, 51] These findings were also supported by monitoring the growth processes in real time by *in situ* synchrotron wide-angle X-ray scattering (WAXS) and ultra-small angle X-ray scattering (USAXS).[51]

The formation of metal dendrites is not limited to synthesis in organic media. For example, Yamauchi *et al.* synthesized Pt dendrites in aqueous media containing Pluronic F127 triblock copolymer and ascorbic acid under ultrasonic irradiation.[47] Their studies showed that the selection of moderate reducing agents such as ascorbic acid and formic acid was critical.[42,46] Pt nanodendrites have been synthesized by similar methods, with a range of nonionic surfactants employed (*e.g.* Brij 700, Tetronic 1107, PVP-co-VA[42], Birj 58[43], poly(vinyl pyrrolidone) (PVP)[44], polyoxyethylene (150) dinonylphenyl ether[45]).

It is worth mentioning that not all branched or dendritic metal nanostructures are created by particle-particle attachment.[56,57] For example, Tilley *et al.* reported the formation of highly branched Pd nanoparticles by reduction of palladium salts under a hydrogen atmosphere.[56] Growth kinetics were monitored by *in situ* X-ray diffraction techniques, which revealed that the branched structure arose from fast overgrowth.[56] Different mechanisms for the synthesis of highly branched nanostructures have been reviewed by Lim and Xia.[58] Importantly, they noted that particle attachment is likely prevalent in many systems but has been overlooked, especially in those which yield single-crystalline dendritic nanostructures on account of oriented attachment.

3. 3. Applications of Single-Component Metal Nanowires and Nanodendrites

The assembly of metal nanoparticles into nanowires or nanodendrites can provide nanostructures with enhanced functionality, particularly for applications in catalysis. Their enhanced properties compared to their 0-D counterparts arise from better electron transport and a decreased tendency toward ripening, dissolution, and aggregation.[13,26,59,60] Network structures of nanowires and nanodendrites can greatly facilitate the transportation of reactants and products in catalytic reactions. Although there are many examples of nanostructures prepared by attachment-based growth being used as catalysts, here we summarize only a few to highlight how the commonly obtained structures can yield enhanced performance.

For example, Chen *et al.* reported enhanced stability and activity from Pt nanochain networks for the oxygen reduction reaction compared to commercial Pt black.[27] This enhancement was attributed to the resistance of robust nanochain networks to ripening. Likewise, Wang *et al.* demonstrated higher activity and durability from unsupported Pt nanowire networks for formic acid and methanol oxidation compare to carbon-supported Pt black.[26] Interestingly, because of their enhanced stability, nanowires and nanodendrites can be used as unsupported nanocatalysts, eliminating the need for a carbon support and corresponding break-down issue.

In the case of alloyed nanostructures, the integration of two metals into one nanostructure can give rise to enhanced catalytic activity, selectivity, and durability though synergistic functions. For example, Yamauchi *et al.* reported the synthesis of dendritic Pt-Ru nanoparticles as a catalyst for methanol oxidation.[61, 62] The incorporation of Ru to the traditionally Pt-only catalyst led to reduced CO poisoning and improved electrocatalytic activity. This enhanced performance arose because oxygen containing species can bind to the oxophilic Ru centers in close proximity to Pt atoms. Such oxygen-containing species can react with adsorbed CO molecules to form CO_2, decreasing the poisoning of intermediate CO. The same group reported enhanced catalytic activity from PdPt alloyed nanodendrites in the electro-oxidation of formic acid.[33]

4. Attachment-based Synthesis of Multicomponent Nanostructures

Section 3 surveyed the single-component metal nanostructures that can arise from attachment-based growth, including nanowires and nanodendrites with enhanced properties for catalysis. However, the attachment mechanism can occur between two crystals with different structures and/or composition. Such coalescence events lead to multicomponent nanostructures. One example is branched core@shell nanostructures. Such structures have been achieved in a number of bimetallic systems, including Au@Pt[63-65], Au@Pd[66-68], Pd@Pt[69-72] and Pd@Rh[73]; however, the formation mechanisms are often unclear, particularly as many early reports disregarded particle-particle attachment. Often, dendritic shells were attributed to heterogeneous nucleation of a second metal on ready-made seeds, with structure-directing agents and kinetic control evoked to account for morphology development. However, real-time TEM imaging studies are clarifying the competition between atomic addition and growth by attachment, with both implicated in the formation of branched nanostructures.[66,69] Sutter *et al.* studied the seeded synthesis of core@shell Au@Pd nanoparticles by *in situ* liquid cell TEM.[67] The electron beam was used not only for imaging but also the source of reducing agent for Pd ions dispersed in solution containing Au seeds. They found that the overgrowth mode was dependent on the size and shape of the Au seeds. Specifically, an increase in the size of icosahedral Au seeds was accompanied with a switch from overgrowth to an attachment mechanism. A continuous Pd shell could be deposited to encapsulate 5 nm Au nanoparticles, whereas dendritic Pd filaments anchored at edge and corners were observed with 30 nm Au nanoparticles, where Pd clusters preferentially attached to under-coordinated sites. This switch was attributed to larger seeds providing less effective sites for atomic addition, leading to higher supersaturation and homogenous nucleation.[67] Likewise, Xia *et al.* also found that both heterogeneous and homogenous nucleation play a role in the formation of core@shell nanodendrites, in this case a Pd@Pt system.[69] Pt bumps heterogeneously nucleated and epitaxially grew on Pd seeds, along with Pt clusters being formed in solution through homogenous nucleation which attached to the growing Pd@Pt structure.[69] Core@shell nanostructures, often with a dendritic periphery, can be obtained in a variety of compositions through particle-particle attachment.[63,64,66-71,73]

In concept, a variety of nanoparticles with different compositions and shapes can be envisioned as building blocks to hybrid structures. The potential of this building block approach is highlighted in a study by Magdassi *et al.* in which the merging of Au nanorods and Ag nanoparticles was examined through both experiment and simulation.[74] They found that Ag behaves as a soft material relative to Au, deforming to wet the Au surface (Figure 6a). A MD simulation of this fusion process found that Ag atoms in peripheral contact are more diffusive with Au atoms, moving toward the Au surface and leading to a wetting-like phenomenon (Figure 6b). This finding is consistent with the lower cohesive energy of Ag compare to Au. In addition, the higher binding energy of Au-Ag compared to Ag-Ag makes the breaking of Ag-Ag bonds and formation of Au-Ag bonds energetically favorable.[74]

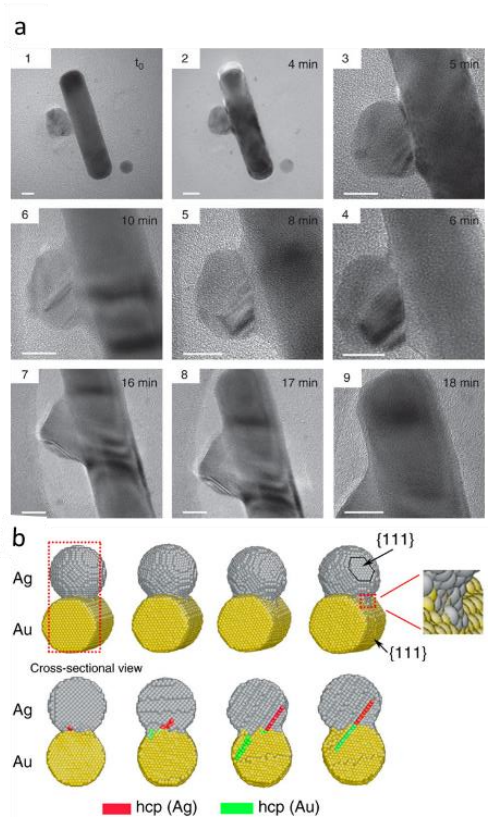

Figure 6. a) Sequential HR-TEM images showing the coalescence of silver nanoparticle with the gold nanorod (scale bars are 10 nm). b) Molecular dynamics simulation of merging an Ag nanoparticle over an Au nanorod at room temperature. Partial dislocations and stacking faults near the interface of Au and Ag are energetically favorable to align up across the interface facilitating the coalescence process. Au and Ag atoms are indicated by yellow and grey balls, respectively. (adapted from Reference 74)

Multicomponent metal nanostructures with high surface areas often show enhanced catalytic activity, selectivity, and durability compared to their monometallic counterparts. Specifically, the core@shell structure contains the main catalyst in the shell and supporting metal in the core. This architecture can reduce precious metal usage when earth-abundant elements are used in the core.[75] Also, the electronic structure of the catalyst can be tuned to enhance activity and reduce catalyst poisoning. This ability arises from induced strain to the shell metal caused by lattice mismatch between the two metals as well as charge transfer between the two metals.[76,77]

For example, Eichhorn *et al.* reported enhanced CO tolerance with dendritic Au@Pt nanoparticles used as a catalyst for oxidation reactions in H_2/CO mixtures.[63] Yang *et al.* also reported high catalytic activity from similar structures but for formic acid oxidation.[68] Xia *et al.* found Pd@Pt nanoparticles to be excellent catalysts for the oxygen reduction and formic acid oxidation reactions.[69,70] Similarly, Yamauchi *et al.* studied the synthesis and catalytic activity of dendritic Au@Pt nanoparticles toward the methanol oxidation reaction.[78] In this example, enhanced catalytic activity was partially attributed to low-coordinated atoms on edges and kinks which could greatly enhance the ability to break C-C bonds in methanol. These examples illustrate that attachment synthesis of multicomponent nanostructures provides new platforms for catalysis.

5. Summary and outlook

The study of oriented and misoriented attachment has attracted a great deal of attention recently in the synthesis of metal nanostructures where attractive dipole interactions, unless induced in capping agents, cannot account for structure formation. As we have highlighted, the main driving force for particle-particle attachment of metals is reduction in surface energy. Moreover, through the use of *in situ* liquid cell TEM, the attachment angle of colliding particles has been identified as a critical parameter that accounts for single-crystalline structures at low contact angles and polycrystalline structures at high angles.

This growth mechanism is enabling a range of metal nanostructures to be achieved, including 1-D nanowires, nanodendrites and nanobundles, dimers, and core@shell structures. Often, these structures are accessed without using any templates. From an application point of view, the synthesis of 1-D and highly branched nanostructures is leading to highly active materials for applications in catalysis. However, given the diversity and complexity of structures that are possible by attachment based growth, new opportunities in sensors, optics, and energy conversion and storage systems may be possible.

Finally, with further development, this method could provide a sustainable and more efficient route to structurally and compositionally complex metal nanostructures. In general, three components are required for the solution phase synthesis of metal nanoparticles: solvent, reducing agent, and stabilizer/structure-directing agent. Recent studies demonstrate attachment-based growth of metal nanostructures in water as an alternative to organic solvents. Moreover, bio-derived reducing agents such as ascorbic acid and formic acid are often used, rather than sodium borohydride or hydrazine. Lastly, as discussed in this review, capping agents are effective in guiding attachment processes through manipulation of surface energies. However, in contrast to overgrowth by atomic addition in which surfactants have a vital role, mechanistic studies reveal that attachment is less dependent on stabilizers. Hence, surfactants may not be required in all cases, and there are several reports of the surfactant-free syntheses of nanostructures based on attachment-based growth.[54,79-81] Insight into the synthetic parameters that drive particle attachment has been coming predominately from *in situ* TEM studies of attachment mechanisms coupled with theoretical modeling. However, because the electron beam can act as a strong reducing agent, many synthetic conditions cannot be

mimicked.[67] Monitoring coalescence and growth processes spectroscopically or through liquid cell synchrotron scattering methods should advance our understanding while maintaining realistic synthetic conditions.[51,56] Better understanding of this approach can pave the way for the cleaner and more sustainable synthesis of metal nanoparticles.

Acknowledgements

This work was supported by Indiana University start-up funds and NSF Award CHE-1306853. SES is a Cottrell Scholar (Research Corporation), Alfred P. Sloan Fellow, and Camille Dreyfus Teacher-Scholar.

References

1. C. M. Cobley, S. E. Skrabalak, D. J. Campbell and Y. Xia, *Plasmonics*, 2009, **4**, 171.
2. H. J. You, S. C. Yang, B. J. Ding and H. Yang, *Chem. Soc. Rev.*, 2013, **42**, 2880.
3. I. M. Al-Akraa, A. M. Mohammad, M. S. El-Deab and B. E. El-Anadouli, *Int. J. Hydrogen Energ.*, 2015, **40**, 1789.
4. S. J. Hwang, S.-K. Kim, J.-G. Lee, S.-C. Lee, J. H. Jang, P. Kim, T.-H. Lim, Y.-E. Sung and S. J. Yoo, *J. Am. Chem. Soc.*, 2012, **134**, 19508.
5. R. Sheldon, in *Green Chemistry in the Pharmaceutical Industry*, ed. P. J. Dunn, A. S. Wells and M. T. Williams, Wiley-VCH Verlag GmbH & Co. KGaA, Weinheim, 2010, ch. 1, pp. 1-20.
6. Y. Xia, Y. J. Xiong, B. Lim and S. E. Skrabalak, *Angew. Chem.-Int. Ed.*, 2009, **48**, 60.
7. R. L. Penn and J. F. Banfield, *Science*, 1998, **281**, 969.
8. H. G. Liao, L. K. Cui, S. Whitelam and H. M. Zheng, *Science*, 2012, **336**, 1011.
9. Z. Aabdin, J. Y. Lu, X. Zhu, U. Anand, N. D. Loh, H. B. Su and U. Mirsaidov, *Nano Lett.*, 2014, **14**, 6639.
10. H. M. Zheng, R. K. Smith, Y. W. Jun, C. Kisielowski, U. Dahmen and A. P. Alivisatos, *Science*, 2009, **324**, 1309.
11. R. L. Penn, *J. Phys. Chem. B*, 2004, **108**, 12707.
12. H. Z. Zhang, J. J. De Yoreo and J. F. Banfield, *ACS Nano*, 2014, **8**, 6526.
13. W. Q. Lv, W. D. He, X. N. Wang, Y. H. Niu, H. Q. Cao, J. H. Dickerson and Z. G. Wang, *Nanoscale*, 2014, **6**, 2531.
14. E. R. Leite and C. Ribeiro, *Crystallization and growth of colloidal nanocrystals*, Springer, New York, 2012.
15. W. D. He, J. H. Lin, X. Lin, N. Lu, M. Zhou and K. H. L. Zhang, *Analyst*, 2012, **137**, 4917.
16. J. H. Liao, Y. Zhang, W. Yu, L. N. Xu, C. W. Ge, J. H. Liu and N. Gu, *Colloid Surf. A-Physicochem. Eng. Asp.*, 2003, **223**, 177.
17. W. Q. Lv, X. M. Yang, W. Wang, Y. H. Niu, Z. P. Liu and W. D. He, *Chemphyschem*, 2014, **15**, 2688.
18. L. Cademartiri and G. A. Ozin, *Adv. Mater.*, 2009, **21**, 1013.
19. C. B. Murray, *Science*, 2009, **324**, 1276.
20. J. M. Yuk, J. Park, P. Ercius, K. Kim, D. J. Hellebusch, M. F. Crommie, J. Y. Lee, A. Zettl and A. P. Alivisatos, *Science*, 2012, **336**, 61.
21. A. Halder and N. Ravishankar, *Adv. Mater.*, 2007, **19**, 1854.
22. H. J. Feng, Y. M. Yang, Y. M. You, G. P. Li, J. Guo, T. Yu, Z. X. Shen, T. Wu and B. G. Xing, *Chem. Commun.*, 2009, 1984.
23. D. F. Zhang, Q. Zhang, L. Y. Niu, L. Jiang, P. G. Yin and L. Guo, *J. Nanopart. Res.*, 2011, **13**, 3923.
24. M. Giersig, I. Pastoriza-Santos and L. M. Liz-Marzan, *J. Mater. Chem.*, 2004, **14**, 607.
25. H. Y. Liang, H. G. Zhao, D. Rossouw, W. Z. Wang, H. X. Xu, G. A. Botton and D. L. Ma, *Chem. Mat.*, 2012, **24**, 2339.
26. B. Y. Xia, H. B. Wu, Y. Yan, X. W. Lou and X. Wang, *J. Am. Chem. Soc.*, 2013, **135**, 9480.
27. J. F. Xu, G. T. Fu, Y. W. Tang, Y. M. Zhou, Y. Chen and T. H. Lu, *J. Mater. Chem.*, 2012, **22**, 13585.
28. Z. C. Zhang, X. Zhang, Q. Y. Yu, Z. C. Liu, C. M. Xu, J. S. Gao, J. Zhuang and X. Wang, *Chem.-Eur. J.*, 2012, **18**, 2639.
29. Z. M. Peng, H. J. You and H. Yang, *ACS Nano*, 2010, **4**, 1501.
30. L. Zhang, J. W. Zhang, Z. Y. Jiang, S. F. Xie, M. S. Jin, X. G. Han, Q. Kuang, Z. X. Xie and L. S. Zheng, *J. Mater. Chem.*, 2011, **21**, 9620.
31. N. Ortiz, R. G. Weiner and S. E. Skrabalak, *ACS Nano*, 2014, **8**, 12461.
32. B. Lim, J. G. Wang, P. H. C. Camargo, C. M. Cobley, M. J. Kim and Y. Xia, *Angew. Chem.-Int. Ed.*, 2009, **48**, 6304.
33. L. Wang and Y. Yamauchi, *Chem.-Asian J.*, 2010, **5**, 2493.
34. Q. Yuan, Z. Y. Zhou, J. Zhuang and X. Wang, *Chem. Mat.*, 2010, **22**, 2395.
35. X. Hong, D. S. Wang, R. Yu, H. Yan, Y. Sun, L. He, Z. Q. Niu, Q. Peng and Y. D. Li, *Chem. Commun.*, 2011, **47**, 5160.
36. L. Yang, C. G. Hu, J. L. Wang, Z. X. Yang, Y. M. Guo, Z. Y. Bai and K. Wang, *Chem. Commun.*, 2011, **47**, 8581.
37. L. H. Shi, A. Q. Wang, T. Zhang, B. S. Zhang, D. S. Su, H. Q. Li and Y. J. Song, *J. Phys. Chem. C*, 2013, **117**, 12526.
38. X. W. Teng, S. Maksimuk, S. Frommer and H. Yang, *Chem. Mat.*, 2007, **19**, 36.
39. X. W. Teng, W. Q. Han, W. Ku and M. Hucker, *Angew. Chem.-Int. Ed.*, 2008, **47**, 2055.
40. X. W. Teng, X. Y. Liang, S. Maksimuk and H. Yang, *Small*, 2006, **2**, 249.
41. J. Y. Chen, T. Herricks and Y. N. Xia, *Angew. Chem.-Int. Ed.*, 2005, **44**, 2589.
42. L. Wang, H. J. Wang, Y. Nemoto and Y. Yamauchi, *Chem. Mat.*, 2010, **22**, 2835.
43. L. Wang and Y. Yamauchi, *Chem.-Eur. J.*, 2011, **17**, 8810.
44. L. Wang and Y. Yamauchi, *Chem. Mat.*, 2009, **21**, 3562.
45. L. Wang, M. Imura and Y. Yamauchi, *ACS Appl. Mater. Interfaces*, 2012, **4**, 2865.
46. L. Wang, C. P. Hu, Y. Nemoto, Y. Tateyama and Y. Yamauchi, *Cryst. Growth Des.*, 2010, **10**, 3454.
47. L. Wang and Y. Yamauchi, *J. Am. Chem. Soc.*, 2009, **131**, 9152.
48. N. V. Long, M. Ohtaki, M. Uchida, R. Jalem, H. Hirata, N. D. Chien and M. Nogami, *J. Colloid Interface Sci.*, 2011, **359**, 339.
49. B. Lim, H. Kobayashi, P. H. C. Camargo, L. F. Allard, J. Y. Liu and Y. Xia, *Nano Res.*, 2010, **3**, 180.
50. N. Ortiz and S. E. Skrabalak, *Angew. Chem.-Int. Ed.*, 2012, **51**, 11757.
51. N. Ortiz, J. A. Hammons, S. Cheong and S. E. Skrabalak, *ChemNanoMat*, 2015, DOI: 10.1002/cnma.201500006.
52. P. Zhou, Z. H. Dai, M. Fang, X. H. Huang, J. C. Bao and J. F. Gong, *J. Phys. Chem. C*, 2007, **111**, 12609.
53. Q. A. Yuan, Z. Y. Zhou, J. Zhuang and X. Wang, *Inorg. Chem.*, 2010, **49**, 5515.
54. X. G. Wen, Y. T. Xie, W. C. Mak, K. Y. Cheung, X. Y. Li, R. Renneberg and S. Yang, *Langmuir*, 2006, **22**, 4836.
55. X. Qin, Z. Y. Miao, Y. X. Fang, D. Zhang, J. Ma, L. Zhang, Q. Chen and X. G. Shao, *Langmuir*, 2012, **28**, 5218.
56. J. Watt, S. Cheong, M. F. Toney, B. Ingham, J. Cookson, P. T. Bishop and R. D. Tilley, *ACS Nano*, 2010, **4**, 396.
57. Y. J. Song, Y. Yang, C. J. Medforth, E. Pereira, A. K. Singh, H. F. Xu, Y. B. Jiang, C. J. Brinker, F. van Swol and J. A. Shelnutt, *J. Am. Chem. Soc.*, 2004, **126**, 635.
58. B. Lim and Y. Xia, *Angew. Chem.-Int. Ed.*, 2011, **50**, 76.
59. M. N. Cao, D. S. Wu and R. Cao, *ChemCatChem*, 2014, **6**, 26.
60. C. Koenigsmann and S. S. Wong, *Energ. Environ. Sci.*, 2011, **4**, 1161.
61. H. Ataee-Esfahani, Y. Nemoto, M. Imura and Y. Yamauchi, *Chem.-Asian J.*, 2012, **7**, 876.
62. H. Ataee-Esfahani, J. Liu, M. Hu, N. Miyamoto, S. Tominaka, K. C. W. Wu and Y. Yamauchi, *Small*, 2013, **9**, 1047.
63. S. G. Zhou, K. McIlwrath, G. Jackson and B. Eichhorn, *J. Am. Chem. Soc.*, 2006, **128**, 1780.
64. Z. Peng and H. Yang, *Nano Res.*, 2009, **2**, 406.
65. H. Ataee-Esfahani, L. Wang and Y. Yamauchi, *Chem. Commun.*, 2010, **46**, 3684.
66. J. Xu, A. R. Wilson, A. R. Rathmell, J. Howe, M. Chi and B. J. Wiley, *ACS Nano*, 2011, **5**, 6119.
67. K. L. Jungjohann, S. Bliznakov, P. W. Sutter, E. A. Stach and E. A. Sutter, *Nano Lett.*, 2013, **13**, 2964.
68. J. S. Han, Z. W. Zhou, Y. Yin, X. T. Luo, J. Li, H. Zhang and B. Yang, *Crystengcomm*, 2012, **14**, 7036.

69. B. Lim, M. J. Jiang, T. Yu, P. H. C. Camargo and Y. Xia, *Nano Res.*, 2010, **3**, 69.
70. B. Lim, M. J. Jiang, P. H. C. Camargo, E. C. Cho, J. Tao, X. M. Lu, Y. M. Zhu and Y. Xia, *Science*, 2009, **324**, 1302.
71. Z. M. Peng and H. Yang, *J. Am. Chem. Soc.*, 2009, **131**, 7542.
72. H. Ataee-Esfahani, M. Imura and Y. Yamauchi, *Angew. Chem.-Int. Ed.*, 2013, **52**, 13611.
73. H. Kobayashi, B. Lim, J. G. Wang, P. H. C. Camargo, T. K. Yu, M. J. Kim and Y. Xia, *Chem. Phys. Lett.*, 2010, **494**, 249.
74. M. Grouchko, P. Roitman, X. Zhu, I. Popov, A. Kamyshny, H. B. Su and S. Magdassi, *Nat. Commun.*, 2014, **5**, 5.
75. S. Zhou, B. Varughese, B. Eichhorn, G. Jackson and K. McIlwrath, *Angew. Chem.-Int. Ed.*, 2005, **44**, 4539.
76. W. J. Tang and G. Henkelman, *J. Chem. Phys.*, 2009, **130**, 6.
77. W. J. Zhou and J. Y. Lee, *Electrochem. Commun.*, 2007, **9**, 1725.
78. H. Ataee-Esfahani, L. Wang, Y. Nemoto and Y. Yamauchi, *Chem. Mat.*, 2010, **22**, 6310.
79. K. R. Krishnadas, P. R. Sajanlal and T. Pradeep, *J. Phys. Chem. C*, 2011, **115**, 4483.
80. Y. C. Han, S. H. Liu, M. Han, J. C. Bao and Z. H. Dai, *Cryst. Growth Des.*, 2009, **9**, 3941.
81. B. Viswanath, S. Patra, N. Munichandraiah and N. Ravishankar, *Langmuir*, 2009, **25**, 3115.

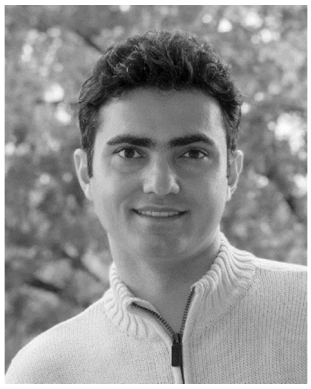

Hamed Ataee-Esfahani received his B.Sc. and M.Sc. in Materials Science and Engineering from Sharif University of Technology and his PhD in Nanoscience and Nanoengineering in 2013 from Waseda University. He is currently a postdoctoral fellow at Chemistry Department of Indiana University. His research interest is focused on shape-controlled synthesis of metal nanoparticles for catalytic and energy applications.

Sara Skrabalak received a B.A. in chemistry from Washington University in St. Louis, conducting research with William Buhro. She then completed her PhD in chemistry from the University of Illinois at Urbana-Champaign under the tutelage of Kenneth Suslick, followed by postdoctoral research at the University of Washington – Seattle with Younan Xia. She is the James H. Rudy Associate Professor of Chemistry at Indiana University – Bloomington and a recipient of NSF CAREER and DOE Early Career Awards. She is a Research Corporation Cottrell Scholar, a Sloan Research Fellow, a Camille-Dreyfus Teacher Scholar, and recipient of the 2014 ACS Award in Pure Chemistry and 2015 Leo Hendrik Baekeland Award.